Journal of Applied Polymer Science

Amelioration of electrochemical and photovoltaic performances on P(VP-*co*-VAc) based gel polymer electrolyte by incorporating double salt for dye-sensitized solar cells

S. Robin, H. M. Ng, S. Ramesh, K. Ramesh

Centre of Ionics University of Malaya, Faculty of Science, Department of Physics, University of Malaya, Kuala Lumpur 50603, Malaysia

Correspondence to: S. Ramesh (E-mail: rameshtsubra@gmail.com)

ABSTRACT: Dye-sensitized solar cell (DSSC) is an alternative photovoltaic application used to replace the liquid electrolyte dependent conventional photovoltaic cell. In this research, gel polymer electrolyte (GPE) was used to replace the unstable liquid electrolyte. This GPE consists of poly[1-vinylpyrrolidone-co-vinyl acetate] (P[VP-*co*-VAc]), tetrabutylammonium iodide (TBAI), sodium iodide (NaI), iodine (I_2), ethylene carbonate (EC), and propylene carbonate (PC). The GPE was tested for its ionic conductivity and an optimum level was reached at sample with 30% TBAI and 6% NaI at 1.17×10^{-3} S cm^{-1}. The DSSC was then fabricated with all GPEs and a photovoltaic performance study was conducted. As a result, the highest photovoltaic conversion efficiency (PCE), η for a single salt was 3.04% for 40% TBAI. When a second salt is added, the system showed improvement in efficiency, η to 4.54% with short circuit current density, J_{sc} of 11.02 mA cm^{-2} and open circuit voltage, V_{oc} of 0.67 V and FF of 61%. The other changes after the addition of TBAI and NaI salts have been observed through X-ray diffraction, Fourier transformation and thermal analysis studies. © 2016 Wiley Periodicals, Inc. J. Appl. Polym. Sci. **2016**, *133*, 43805.

KEYWORDS: blends; dielectric properties; electrochemistry; infrared spectroscopy; thermogravimetric analysis

Received 20 December 2015; accepted 17 April 2016

DOI: 10.1002/app.43805

INTRODUCTION

Dye-sensitized solar cell (DSSC) was first introduced to the world by Michael Gratzel in 1991 as a low-cost alternative to conventional method of producing electricity.[1] A DSSC is made up of an electrolyte containing an iodide/triiodide redox mediator inserted in between two electrodes, i.e., the titanium dioxide (TiO_2) coated conducting electrode and a platinum (Pt) counter electrode.[2] Studies show that liquid electrolyte based DSSCs can produce efficiency exceeding 12%.[3] However, liquid electrolyte has few practical problems in long term due to its volatility and has major stability problem as a result of leakage, flammability of the liquid and decomposition of the dye.[4,5] Thus, researchers propose to substitute the liquid electrolyte with a quasi-solid polymer electrolyte or also known as gel polymer electrolyte (GPE).[6–10]

GPEs have reasonably good ionic conductivity, low vapor pressure, tremendous filling, and contacting properties and better thermal stability to make it a good electrolyte relative to liquid electrolytes. Nonetheless, GPE has its own setbacks. It has poor efficiency and low ionic conductivity. Probably, this is caused by the microscopic nature of the GPE, whereby its intermolecular spacing is much smaller compared to liquid electrolyte. Thus, hindering the free flow of ions.[11]

The usage of copolymer is a great way to improvise the disadvantages of GPE. Copolymer such as poly(vinyidene fluoride-*co*-hexafluoro propylene) (PVdf-HFP) can add stability to an electrolyte. This is because the HFP is amorphous in nature which helps to trap large amount of ions, and crystalline form PVdf enhances the mechanical strength for the copolymer.[12] Research has also proven that PVdf-HFP GPEs has higher ionic conductivity at room temperature as compared to other polymers.[13] Our previous study has shown that copolymer (like P[VP-*co*-VAc]) based GPE has high potential as the host polymer for the electrolytes of a DSSC. The DSSC fabricated with P[VP-*co*-VAc]) based GPE that was incorporated with single salt and ionic liquid shows an efficiency of 4.67%.[14]

Recent studies show that the efficiency of DSSCs can be improved by adding second salts, i.e., the combination of small and large cations, than the corresponding single salt.[15] In this study, instead of using ionic liquid as what was done in previous study, we tried to incorporate two different salts into the P[VP-*co*-VAc]) based GPE in order to study the performances of a double salt system

Table I. The composition of P(VP-*co*-VAc) Based Single Salt GPEs System

Electrolyte	TBAI (%)	P(VP-co-VAc) (g)	TBAI (g)	I_2 (g)	EC (g)	PC (g)
O	0	5.0000	0	0	1.5	1.5
A	10	4.4200	0.5	0.0765	1.5	1.5
B	20	3.8470	1.0	0.1530	1.5	1.5
C	30	3.2705	1.5	0.2295	1.5	1.5
D	40	2.6940	2.0	0.3060	1.5	1.5

based P[VP-*co*-VAc]) GPE. Iodide salts such as NaI, LiI, and KI are made up of small cations, i.e., Na^+, Li^+, and K^+, respectively. These cations contribute toward better photogeneration of electron and allow faster diffusion at the dye. Hence, it can be absorbed easily by the TiO_2 electrode. Meanwhile, the bulkier cations, i.e., TPA^+ and TBA^+ would assist in the enlargement of the separation of the polymer matrix. The changes in the efficiency can be discovered by analysing the short circuit current density and ionic conductivity.[16,17] Thus, in this study, instead of using the ionic liquid, we sought to study the performance of the P[VP-*co*-VAc] based GPE incorporated with two different salts.

In this research, the working electrode, i.e., FTO glass with TiO_2 and di-tetrabutylammonium cis-bis (isothiocyanato) bis (2,2′-bipyridyl-4,4′-dicarboxylato) ruthenium (II) [N-719] dye, and the counter electrode, i.e., FTO glass coated with Pt together with GPE was fabricated to form the DSSC. The GPE was made up of P(VP-*co*-PVAc), tetrabutylammonium iodide (TBAI), sodium iodide (NaI), iodine (I_2), ethylene carbonate (EC), and propylene carbonate (PC). The ionic conductivity, temperature dependence, and efficiency test were carried out for the DSSC.

EXPERIMENTAL

Materials

P(VP-*co*-VAc), TBAI, NaI, and N-719 dye were all purchased from Sigma-Aldrich whereas I_2, EC, and PC were purchased from Schmidt Chemicals.

Preparation of Photoelectrodes

The electrode was prepared by coating TiO_2 paste on the FTO glass. TiO_2 was synthesized by grounding the mixture of 0.5 g TiO_2 powder (P-25), 2 mL nitric acid (pH = 2), and Triton X-100. After applying it on the FTO glass, it was spun in a rotating machine to ensure even coating. Then, it was sintered for 30 min at 450 °C. Finally, it was immersed in a Ruthenium dye solution for 24 h prior to use.

Preparations of Pt Counter Electrodes

This counter electrode is prepared by applying hexachloroplatinic acid solution (H_2PtCl_6) and isopropyl alcohol (C_3H_7OH) at 1:1 ratio on the conducting surface of the FTO glass. It was then air-dried with fan and results in a coating. The subsequent coating was sintered at 100 °C for 5 min continued by 500 °C for 30 min. This results in a first tier Pt coating. Finally, it was washed with ethanol. The process was repeated twice for even coating.

Preparation of Gel Polymer Electrolyte

The GPE was prepared by using of EC, PC, Iodine, TBAI, NaI, and P(VP-*co*-VAc). The experiment was separated into two systems, i.e., single salt (first) system and double salt (second) system. The composition was shown in Tables I and II, respectively.

For the first system, the EC and PC ratio used was 1:1. The weights of all chemicals are varied according to the composition. Iodine was added as to one tenth of total mole amount of the iodine salts. The composition of each samples is shown in Table I. Appropriate amounts of EC, PC, I_2, and TBAI were dissolved in a closed bottle using a magnetic stirrer. The copolymer was then added batch by batch. They were continuously stirred at 80 °C until complete dissolution. The process was repeated for other sets of compositions.

In the second system, the composition of electrolyte from the first system with best ionic conductivity and efficiency will be selected for the addition of the second salt, NaI. The double salt electrolyte was prepared for different compositions of NaI as shown in Table II.

Ionic Conductivity of Gel Polymer Electrolytes

An electrochemical impedance spectroscopy study was conducted to obtain the ionic conductivity of each GPE sample. A computer connected to an impedance analyzer called Hioki 3532-50 LCR Hi-Tester was used for this measurement from the frequency range of 50 Hz to 1 MHz. The ionic conductivity of each sample was calculated using the equation:

$$\sigma = l/R_b A \quad (1)$$

where σ is the ionic conductivity in S/cm, l is thickness of the sample in cm, R_b is the bulk resistance in Ω, and A is the

Table II. Composition of P(VP-*co*-VAc) Based Double Salt GPE System

Electrolyte	NaI (%)	P(VP-co-VAc) (g)	TBAI (g)	NaI (g)	I_2 (g)	EC (g)	PC (g)
C1	3	3.1469	1.455	0.15	0.2481	1.5	1.5
C2	6	3.0290	1.401	0.30	0.2700	1.5	1.5
C3	9	2.8999	1.365	0.45	0.2851	1.5	1.5
C4	12	2.7763	1.32	0.60	0.3037	1.5	1.5

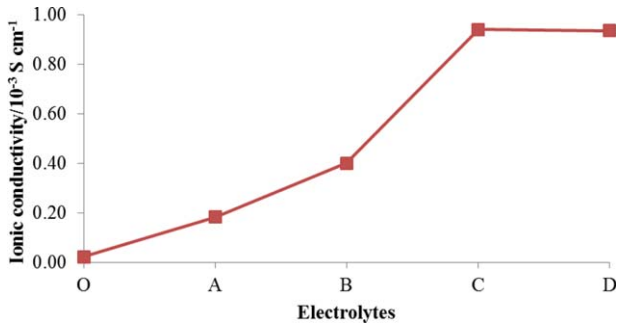

Figure 1. Variation of ionic conductivity as a function of different samples of GPE with single salt system at room temperature. [Color figure can be viewed in the online issue, which is available at wileyonlinelibrary.com.]

surface area of the stainless steel disc. The sample was sandwiched between two stainless steel electrodes. The sample was tested for its EIS at room temperature and a range from 30 to 100 °C at 10 °C interval. The ionic conductivity for each sample in accordance to its temperature is shown in Figure 1.

DSSC Characterization

The DSSCs were fabricated by sandwiching the GPE in the configuration of FTO/TiO_2/Dye/electrolyte/Pt/FTO. The J-V characteristics of the DSSC were measured under the illumination of 100 mW cm^{-2} simulated sunlight, from a Newport LCS-100 Series solar simulator, with a Metrohm Autolab potentiostat (PGSTAT128N). Electrochemical impedance spectroscopy measurements were carried out in the range of 0.1 to 100,000 Hz with AC potential of 0.01 V. A potential bias equal to open circuit voltage was applied.

RESULTS AND DISCUSSION

EIS Studies on Gel Polymer Electrolytes

The efficiency of DSSC is highly dependent on the iodide ionic conductivity of its electrolyte. This is mainly due to mobility of redox couple.[18] Generally, the ionic conductivity is affected by the number of charge carrier. On the other hand, at high concentration of salt added, it is widely dependent on the mobility of ions.[19,20] The ionic conductivity of different GPE compositions was studied by plotting a graph of ionic conductivity against different salt percentages as in Figures 1 and 2.

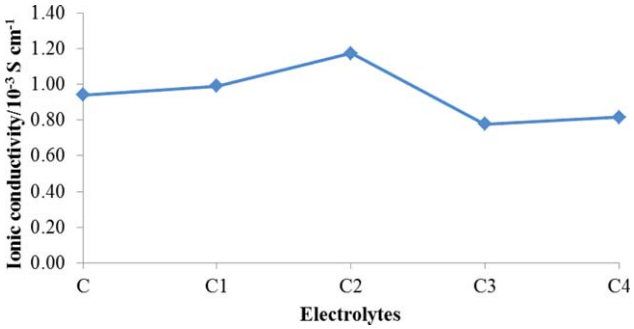

Figure 2. Variation of ionic conductivity as a function of different samples of GPE with double salt system at room temperature. [Color figure can be viewed in the online issue, which is available at wileyonlinelibrary.com.]

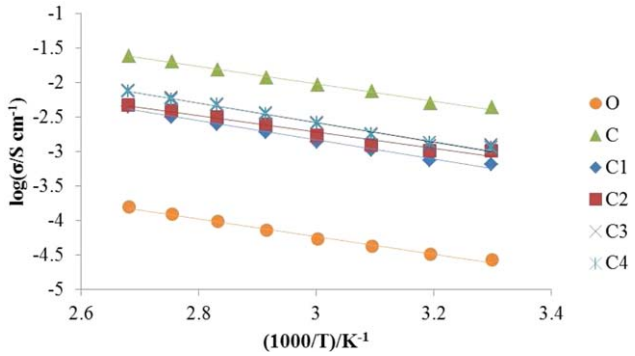

Figure 3. Arrhenius plots for the conductivity of GPE samples. [Color figure can be viewed in the online issue, which is available at wileyonlinelibrary.com.]

The ionic conductivity was calculated using eq. (1). As seen in Figure 1, the ionic conductivity increased in accordance with the weight percentage of TBAI salt added until it reached its peak at TBAI sample C with 0.94 mS cm^{-1}. The increase in ionic conductivity was mainly due to the extra charge carriers from the salt, TBAI which had TBA^+ cation and I^- anions.[21] Although electrolytes C and D have almost the same ionic conductivity, electrolyte C was preferred to be added with the second salt, i.e., NaI. This is due the physical property of electrolyte D, which was more liquid in nature compared to C. Since, this research is focused on GPEs, thus justifies the selection of electrolyte C. As per ionic conductivity efficiency, both C and D differ by ~0.09%, which is quite insignificant. The amount of NaI added can be seen in Table II. The highest conductivity was obtained at NaI sample C2 with 1.17 mS cm^{-1} conductivity. This conductivity is more than that of any composition of single salt.

This happens largely due to the size of ions from both salts. Generally, TBA^+ is much more bulky compared to Na^+ ion. Large ions such as TBA^+ will inhibit the flow of ions. As more NaI added, it replaces the TBAI. Thus, the dissociated Na^+ and I^- ions will have huge contribution to the ionic conductivity of GPE due to increase mobile Na^+ ions compared to the large TBA^+ ions. From both systems, it was understood that there was a decrease in ionic conductivity after the addition of optimum salt content. This occurs due to clumping of ions. When more salt is added, there will be excess dissociated cations and anions. These excess ions lead to the formation of ion pairs. These ion pairs are neutral and cause mobile ions to reduce. When more of these ion pairs form, they group together and become like a barrier to restrict the free flow of ions, eventually reducing the ionic conductivity.[22,23]

The temperature dependence of the GPE samples was studied by measuring the ionic conductivity from 30 to 100 °C. The graph was plotted as in Figure 3 and it displays Arrhenius behavior with a regression value of ~0.97. The Arrhenius equation is as below[24]:

$$\sigma T = B \exp\left(-\frac{E_a}{kT}\right) \quad (2)$$

where σ is the ionic conductivity, B is the preexponential factor, k is the Boltzman constant, E_a is activation energy, and T is the

Table III. The Activation Energy of GPE Samples at Different Concentration of TBAI and NaI Salts

Electrolytes	Activation energy, E_a (kJ mol^{-1})
O	1.465
A	1.439
B	1.399
C	1.254
D	1.245
C1	1.375
C2	1.187
C3	1.404
C4	1.381

temperature. Such Arrhenius behavior occurs mainly due to the hopping of ion from one site to another site. When, heat is applied to the GPE, the ions accumulate it until threshold heat energy, where it incites the hopping of ion. This threshold energy is called the activation energy, E_a. At this moment, the ions are mobile enough to flow.[25] By understanding this, we can deduce that, GPEs with lower E_a will have better ionic conductivity since the ions require lesser energy to hop or move freely within the polymer matrix.[26] The E_a can be determined by measuring the slope of the trend line for each graph. The E_a for different GPEs are shown in the Table III.

Thermogravimetric Analysis of GPE Samples

The thermogravimetric analysis (TGA) was conducted for different samples from 20 to 700 °C and the thermograms is shown in Figure 4. The degradation temperature of the pure P(VP-*co*-VAc), sample P(VP-*co*-VAc) with EC:PC, sample C, sample C2 and sample C3 was tabulated in Table IV. Initially, there was about 2–7% weight loss in all samples from 30 to 100 °C. This was probably due to the evaporation of moisture absorbed, solvents, and/or low molecular weight impurities in the samples.[31] There was even weight loss going on from ~100 to 200 °C. This was mostly due to the evaporation of EC, PC, and some I_2 in the GPEs. Although EC and PC have high boiling point, it did evaporate at a lower temperature below its boiling point, and such similar trend was reported by Kim *et al.*[32]

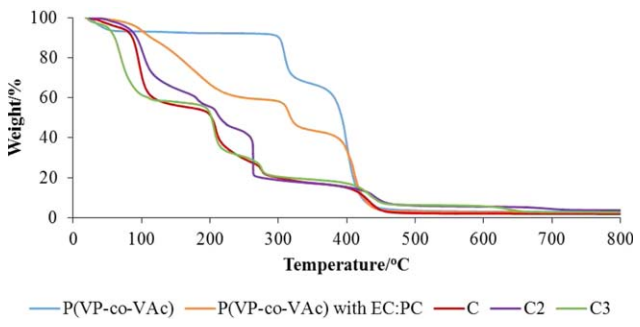

Figure 4. Thermogravimetric analysis of pure P(VP-*co*-VAc) and GPE samples C, C2, and C3. [Color figure can be viewed in the online issue, which is available at wileyonlinelibrary.com.]

Table IV. The Degradation Temperature of Pure P(VP-*co*-VAc) and Different GPE Samples

Samples	$T_{max(PVAc)}$	$T_{max(PVP)}$
P(VP-co-VAc)	302	388
P(VP-co-VAc) with EC:PC	308	398
C	273	416
C2	262	415
C3	270	418

Then on, the pure P(VP-*co*-VAc) had two major drop in weight, i.e., at degradation temperature, $T_{max(PVAc)}$ = 302 °C and $T_{max(PVP)}$ = 388 °C. The drop at $T_{max(PVAc)}$ was mainly due to the deacytylation of PVAc and at $T_{max(PVP)}$ was due to the breakdown of PVP.[33,34] Further degradation temperature for P(VP-*co*-VAc) with EC:PC, 30 wt % TBAI, 6 wt % NaI, and 9 wt % NaI were tabulated in the table above. As observed, the $T_{max(PVAc)}$ for the GPEs decreased upon addition of TBAI and NaI. Meanwhile, the $T_{max(PVP)}$ for sample C, C2, and C3 increases with the addition of the salts. This suggests that the addition of salt decreases the thermal stability at the PVAc region and increases the thermal stability at the PVP region in this GPE systems. Although adding salts decrease the decomposition temperature of the GPE, it still has its own advantage. Lower degradation temperature means, the backbone of the polymer tends to be softer. Hence, less energy is needed to break down the polymer to achieve amorphous state. This idea is backed by results obtained from the XRD analysis.

FTIR Measurements of GPEs

Fourier Transform Infrared (FTIR) spectroscopy is a very important technique in the exploration of the interaction among the individual materials in a polymer electrolytes system. The FTIR spectra of the pure P(VP-*co*-VAc), pure TBAI, pure NaI, sample C, and sample C3 were shown in Figure 5. Few of the main absorption bands of P(VP-*co*-VAc) can be observe at

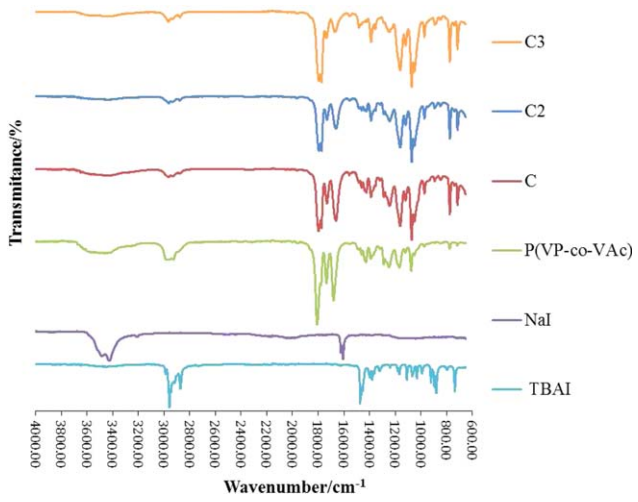

Figure 5. FTIR spectra of pure TBAI, pure NaI, pure P(VP-*co*-VAc), and the GPE samples C, C2, and C3. [Color figure can be viewed in the online issue, which is available at wileyonlinelibrary.com.]

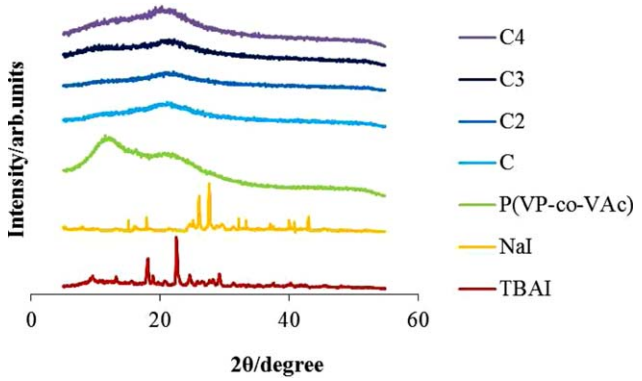

Figure 6. XRD patterns of pure TBAI, pure NaI, pure P(VP-*co*-VAc), and the GPE samples with different concentration of salts. [Color figure can be viewed in the online issue, which is available at wileyonlinelibrary.com.]

3600–3000, 3000–2800, 1446, and 1300–1000 cm^{-1}. They were attributed with the O–H stretching, C–H stretching, C–N stretching, and C–O–C stretching, respectively. Meanwhile, the vibrational bands observed at 1380 and 775 cm^{-1} were ascribed to C–H bending and C–H wagging of the PVAc region, respectively. On the other hand, the C–H bending, C–CH_2 stretching, C–C stretching, and CH_2 bending of the PVP region can be seen at 1443, 1171, 972, and 846 cm^{-1}, respectively.[27,28]

The addition of the two salts into the polymer host results in complexation between the salt and the polymer matrix. This interaction could have influence the structure of the polymer back bones and affecting the charge mobility of the polymer matrix. It can be seen from the shifting of the strong bands of the C–O stretching of PVAc and PVP which peaks at 1731 and 1671 cm^{-1} of the pure P(VP-*co*-VAc) spectrum. After the addition of TBAI (sample C), these two strong band can be seen shifted to a different wave numbers which peaks at 1735 and 1665 cm^{-1}, respectively. Furthermore, after the addition of NaI into the system, the intensity of these two peaks is found to be lesser. The shifting in peaks and reduce in the intensity imply that the C=O group is acting as a strong electron donor which could interacts with the TBA^+ and Na^+ ions. Similar ion interactions of the carbonyl group with the cations have also been reported in a few literatures. Meanwhile, the band appear at 1247 cm^{-1} of the pure P(VP-*co*-VAc) which is attributed to the important C–N stretching band can be observed shifted to lower wavelengths of 1241 and 1242 cm^{-1} for sample C and C3, respectively. This is due to the interactions of the N atom of C–N of the P(VP-*co*-VAc) with the I− of the two salts. The N atom has a strong withdrawing tendency character and it appears that the N atom in the PVP region are attracting the I− and causes shifting of the C-N band in sample C, C2 and sample C3.[29,30] From the shifting that can be observed, it is assumed that the Na+ and TBA+ cations is interacting with the oxygen atom of both PVP and PVAc region while the I− is interacting with the N atom of the PVP region.

XRD Analysis of GPE Samples

XRD studies for the pure TBAI, P(VP-*co*-VAc), sample C, C2, and C3 were performed and the results were shown in Figure 6. As observed in Figure 6, the sharp diffraction peaks that could be seen in the pure NaI and TBAI spectrums indicate the crystalline nature of the salts.[35] The disappearance of these sharp diffractions in sample C, C2, and C3 indicates the complete dissolution of the salts in the polymer matrix and there were not any excess of salts in these samples. Zhang *et al.* has mentioned that if this phenomenon or trend can be seen, this could shows that some complexation has occurred in between the polymers and the two other salts.[36]

As for the spectrum of pure P(VP-*co*-VAc), the broad diffraction peaks which appear at 2θ = 12° corresponding to pure PVAc and 2θ = 21° corresponding to pure PVP. The broad peaks indicate that the polymer exhibits an amorphous phase. Upon addition of salt, these peaks were seen to become flatter. Thus, it is believed that the TBAI and NaI have reduced the crystallinity and in turn increased the amorphousness of the GPE. However, the addition of more salts, i.e., above the optimum level will probably not increase the amorphous nature. Instead, it might induce the crystalline peak due the recrystallization of salt as seen in sample C4.[37]

Addition of salts into the polymer host will result in interaction or also known as complexion with the host polymer matrix. This will significantly influence the local structure of the polymer backbone and affects its mobility. In this context, addition of salt improves the mobility of charge carriers/ion due to the amorphous nature of the GPE. By improving the mobility, it will help increase the ionic conductivity and hence improvise the efficiency of the GPE. This truly reflects on the ionic conductivity result as 6 wt % which is the more amorphous in nature having highest ionic conductivity.[38]

Photovoltaic Performances and EIS Studies of DSSCs

The photocurrent-photovoltage (*J-V*) characteristics for all samples are measured but only six significant curves for the DSSCs are shown in the Figure 7. The values of open circuit voltage

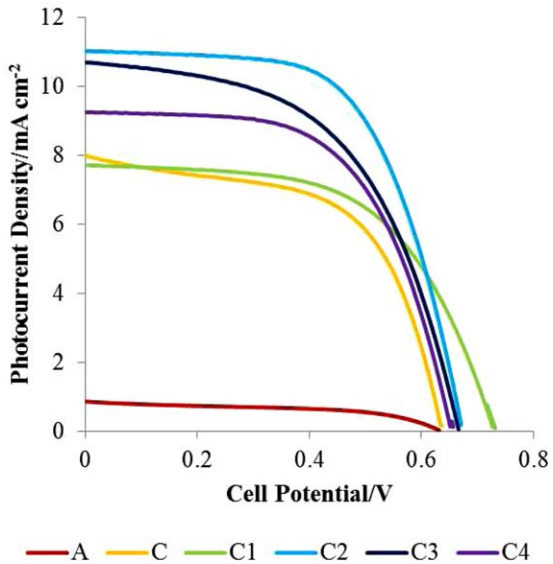

Figure 7. The photocurrent-photovoltage (*J-V*) characteristics of the GPE samples consisting of different concentration of the TBAI and NaI salts. [Color figure can be viewed in the online issue, which is available at wileyonlinelibrary.com.]

Table V. Photovoltaic Parameters of the GPE Samples Consisting of Different Composition

Electrolyte	J_{sc} (mA cm^{-2})	V_{oc} (V)	FF (%)	η (%)
A	0.85	0.63	51	0.28
B	4.12	0.65	58	1.55
C	7.99	0.64	58	2.95
D	7.12	0.66	65	3.04
C1	7.70	0.73	57	3.24
C2	**11.02**	**0.67**	**61**	**4.54**
C3	10.69	0.67	53	3.80
C4	9.24	0.66	59	3.59

Bold values are indicate best performing sample.

(V_{oc}) and the short circuit current density (J_{sc}) were measured and the fill factor (FF) and efficiency (η) were calculated. The results are tabulated in Table V. As known in advance, ionic conductivity is an important measure that influences the DSSCs performance. Nevertheless, there are some other factors that affect the efficiency of DSSCs, i.e., the cation.[39] The interaction between cation and the TiO_2 causes a positive shift of the flat band potential of the semiconductor and formation of deeper states of electron-trapping. These electron-trapping states are important for the electron transfer to the current collector.[40] Small cation such as Na^+ can easily absorbed into the nanoporous TiO_2 grain structure compared to the much bulkier cation, TBA^+. This will induce a positive shift of the conduction band edge potential and eventually increases the J_{sc}. Although the bulkier TBA^+ cation has smaller positive conduction band shift,

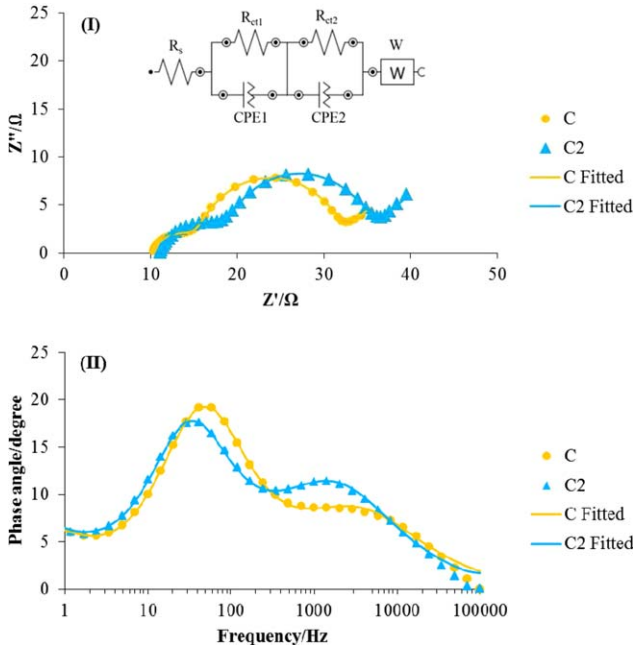

Figure 8. Electrochemical impedance spectra of DSSCs fabricated with sample C and C2 in the form of (I) Nyquist plot and (II) Bode phase plot under the illumination of 100 mW cm^{-2}. [Color figure can be viewed in the online issue, which is available at wileyonlinelibrary.com.]

Table VI. Parameters of the Equivalent Circuits for the EIS Data of the DSSCs

Electrolyte	R_s (Ω)	R_{ct1} (Ω)	R_{ct2} (Ω)	W ($S^{1/2}$ Ω^{-1})
C	10.2	11.4	14.9	90.5
C2	11	8.05	16.7	66.8

it still produce high number of iodide ion due to its high dissociation rate.[41,42] Thus, this proves that double cation system can improve the ionic conductivity, which then increases the J_{sc} and effectively increasing the efficiency. In this research, the electrolyte C2 (as highlighted in Table V) shows the highest efficiency (4.54%) with the highest J_{sc}, 11.02 mA cm^{-2}. This verifies that J_{sc} is directly related to efficiency.

Figure 8(I) shows the results of the impedance measurements and the fitted data of the DSSCs fabricated with single salt and double salt system (C and C2). The parameter used to fit the curves were listed in Table VI. The response at higher frequency shows the charge transfer resistance at Pt counter electrode and denoted as R_{ct1} while the middle-frequency region denoted as R_{ct2} correspond to the electron transport that occurred in the mesoporous TiO_2 layer and the back reaction of the TiO_2 and electrolyte interface. The spike that was found below 10 Hz was attributed to the Warburg diffusion (W) of the I_3^-/I^- in the electrolyte which has the parameter of Y0 ($S^{1/2}$ Ω^{-1}). R_s is basically the ohmic serial resistance of the sheet resistance of the FTO and it could be found at the intersection of the *x*-axis and the high-frequency semicircle. In Figure 8, three arcs were observed in the Nyquist plots and R_{ct2} is where it mainly defines the recombination processes of the electrons in the TiO_2 layer and the electrolyte interface. The addition of the second salt, NaI reduces the impedance component at R_{ct2} indicating that the addition of the Na^+ cations increases the surface resistance at this interface and thus decreases the charge recombination processes. This can be further confirmed in the Bode plots. In EIS theory, the character frequency in the middle frequency which is where R_{ct2} was found is inversely proportional to the electron lifetime. As seen in Figure 8(II), the middle-frequency peak was found to be shifted to lower frequencies indicating that the addition of the NaI salt elongates the electron lifetime at this interface. This could be the reason for the slight increase of the open circuit voltage of the cell after the addition of the second salt, NaI.

CONCLUSIONS

There was performance improvement for DSSC with double salt GPE of TBAI and NaI by using copolymer P(VP-*co*-VAc). The ionic conductivity of the double salt GPE increases with increasing NaI until it reached its peak or optimum conductivity of 1.17×10^{-3} S cm^{-1} for 30 wt % TBAI and 6 wt % NaI. All samples followed Arrhenius behavior and showed a trend of decreasing E_a with increasing ionic conductivity. The highest efficiency was obtained for the same GPE sample which was 4.54% with J_{sc} of 11.02 mA cm^{-2}, V_{oc} of 0.67 V, and FF of 61%.

ACKNOWLEDGMENTS

Authors would like to appreciate financial support by grant number PG034-2013A from Institute of Research Management and Monitoring (IPPP) and FP012-2015A from Fundamental Research Grant Scheme (FRGS) of University of Malaya.

REFERENCES

1. Regan, B. O.; Gratzel, M. *Nature* **1991**, *353*, 737.
2. Arof, A. K.; Aziz, M. F.; Noor, M. M.; Careem, M. A.; Bandara, L. R. A. K.; Thotawatthage, C. A.; Rupasinghe, W. N. S.; Dissanayake, M. A. K. L. *Int. J. Hydrogen Energy* **2013**, *6*, 2929.
3. Aswani, Y.; Lee, H. W.; Nok, T. H.; Chenyi, Y.; Kumar, C. A.; Khaja, N. M. *Science* **2011**, *334*, 629.
4. Lan, Z.; Wu, J.; Lin, J.; Huang, M.; Li, P.; Li, Q. *Electrochim. Acta* **2008**, *53*, 2296.
5. Wang, P.; Wenger, B.; Humphry-Baker, R.; Moser, J. E.; Teuscher, J.; Kantlehner, W.; Mezger, J.; Stoyanov, E. V.; Zakeeruddin, S. M.; Grätzel, M. *J. Am. Chem. Soc.* **2005**, *127*, 6850.
6. Wang, P.; Zakeeruddin, S. M.; Moser, J. E.; Nazeeruddin, M. K.; Sekiguchi, T.; Gratzel, M. *Nat. Mater.* **2003**, *2*, 402.
7. Wu, J.; Lan, Z.; Wang, D.; Hao, S.; Lin, J.; Huang, Y.; Yin, S.; Sato, T. *Electrochim. Acta* **2006**, *51*, 4243.
8. Suryanarayanan, V.; Lee, K. M.; Ho, W. H.; Chen, H. C.; Ho, K. C. *Sol. Energy Mater. Sol. Cells* **2007**, *91*, 1467.
9. Lim, S. J.; Kang, Y. S.; Kim, D. W. *Electrochim. Acta* **2011**, *56*, 2031.
10. Wang, M.; Pan, X.; Fang, X. Q.; Guo, L.; Zhang, C. N.; Huang, Y.; Huo, Z. P.; Dai, S. Y. *J. Power Sour.* **2011**, *196*, 5784.
11. Lai, Y. H.; Chiu, C. W.; Chen, J. G.; Wang, C. C.; Lin, J. J.; Lin, K. F. *Sol. Energy Mater. Sol. Cells* **2009**, *93*, 1860.
12. Xing, G. Z.; En, M. J.; Gu, H. B. *Appl. Surf. Sci.* **2013**, *287*, 8.
13. Suryanarayanan, V.; Lee, K. M.; Ho, W. H.; Chen, H. C.; Hoa, K. C. *Sol. Energy Mater. Sol. Cells* **2007**, *91*, 1467.
14. Ng, H. M.; Ramesh, S.; Ramesh, K. *Electrochim. Acta* **2015**, *175*, 169.
15. Agarwala, S.; Thummalakunta, L. N. S. A.; Cook, C. A.; Peh, C. K. N.; Wong, A. S. W.; Keb, L.; Ho, G. W. *J. Power Sour.* **2011**, *196*, 1651.
16. Dissanayakea, M. A. K. L.; Jayathissa, R.; Seneviratne, V. A.; Thotawatthage, C. A.; Senadeera, G. K. R.; Mellander, B. E. *Solid State Ionics* **2014**, *265*, 85.
17. Dissanayake, M. A. K. L.; Rupasinghe, W. N. S.; Seneviratne, V. A.; Thotawatthage, C. A.; Senadeera, G. K. R. *Electrochim. Acta* **2014**, *145*, 319.
18. Kim, Y. J.; Bach, J. H.; Cheng, Y. B.; Caruso, R. A. *Appl. Phys. Lett.* **2014**, *145*, 213510.
19. Yu, B.; Zhou, F.; Wang, C.; Liu, W. *Eur. Polym. J.* **2007**, *43*, 2699.
20. F. M. Gray, Solid Polymer Electrolytes: Fundamentals of Technological Applications, Wiley-VCH: UK; **1991**, pp 83–93.
21. Singh, P. K.; Kim, K. W.; Park, N. G.; Rhee, H. W. *Synth. Met.* **2008**, *158*, 590.
22. Rajendran, S.; Babu, R. S.; Sivakumar, P. *J. Power Sour.* **2007**, *170*, 460.
23. Liang, Y. H.; Wang, C. C.; Chen, C. Y. *Eur. Polym. J.* **2008**, *44*, 2376.
24. Fleshman, A. M.; Petrowsky, M.; Jernigen, J. D.; Bokalawela, R. S. P.; Johnson, M. B.; Frech, R. *Electrochim. Acta* **2011**, *57*, 147.
25. Ramesh, S.; Ng, H. M.; Shanti, R.; Ramesh, K. *Plast. Technol. Eng.* **2013**, *52*, 1474.
26. Yang, C. C.; Yang, J. M.; Wu, C. Y. *J. Power Sour.* **2009**, *191*, 669.
27. Stephen, A. M.; Saito, Y.; Muniyandi, N.; Ranganathan, N. G.; Kalyanasundaram, S.; Elizabeth, R. N. *Solid State Ionics* **2002**, *148*, 467.
28. Kim, K. S.; Park, S. Y.; Yeon, S. H.; Lee, H. *Electrochim. Acta* **2005**, *50*, 5673.
29. Bianco, G.; Soldi, M. S.; Pinheiro, E. A.; Pires, A. T. N.; Gehlen, M. H.; Soldi, V. *Polym. Degrad. Stab.* **2003**, *80*, 567.
30. McNeill, I. C.; Ahmed, S.; Memetea, L. *Polym. Degrad. Stab.* **1995**, *48*, 89.
31. Ravi, M.; Kumara, K. K.; Mohan, V. M.; Rao, V. V. R. N. *Polym. Test.* **2014**, *33*, 152.
32. Ulaganathan, M.; Pethaiah, S. S.; Rajendran, S. *Mater. Chem. Phys.* **2011**, *129*, 471.
33. Ravi, M.; Pavani, Y.; Kumar, K. K.; Bhavani, S.; Sharma, A. K.; Rao, V. V. R. N. *Mater. Chem. Phys.* **2011**, *130*, 442.
34. Ramya, C. S.; Selvasekarapandian, S.; Savitha, T.; Hirankumar, G.; Angelo, P. C. *Physica B* **2007**, *393*, 11.
35. Bhargav, P. B.; Mohan, V. M.; Sharma, a. K.; Rao, V. V. R. N. *Ionics* **2007**, *13*, 173.
36. Zhang, R.-K.; Sun, Z.; Xie, H.-H.; Wu, X.; Liang, M.; Xue, S. *Sol. Energy* **2012**, *86*, 2346.
37. Noor, M. M.; Buraidah, M. H.; Careem, M. A.; Majid, S. R.; Arof, A. K. *Electrochim. Acta* **2014**, *121*, 159.
38. Prajapati, G. K.; Gupta, P. N. *Physica B* **2011**, *406*, 3108.
39. Bandara, T. M. W. J.; Jayasundara, W. J. M. J. S. R.; Dissanayake, M. A. K. L.; Fernando, H. D. N. S.; Furlani, M.; Albinsson, I.; Mellander, B. E. *Int. J. Hydrogen Energy* **2014**, *39*, 2997.
40. Kelly, C. A.; Farzad, F.; Thompson, D. W.; Stipkala, J. M.; Meyer, G. J. *Langmuir* **1999**, *15*, 7047.
41. Brennan, L. J.; Barwich, S. T.; Satti, A.; Faure, A.; Gun'ko, Y. K. *J. Mater. Chem. A* **2013**, *1*, 8379.
42. Cha, S. Y.; Lee, Y. G.; Kang, M. S.; Kang, Y. S. *J. Photochem. Photobiol. A* **2010**, *211*, 193.